

403505

CATALOGED ASIA  
A. AD 116

OFFICE OF NAVAL RESEARCH

Number 3511 (00)

Project Number 051 - 380

EXPERIMENTAL INVESTIGATIONS ON THE LIGHT SCATTERING OF COLLOIDAL SPHERES.  
V. DETERMINATION OF SIZE DISTRIBUTION CURVES BY MEANS OF SPECTRA OF THE  
SCATTERING RATIO

BY

W. HELLER, M. L. WALLACH, AND A. F. STEVENSON

TECHNICAL REPORT NO. 4 (50)

April 15, 1963

Submitted by

W. Heller, Project Director

Department of Chemistry

Wayne State University

Detroit 2, Michigan

DDC  
MAY 15 1963

ASIA A

Reproduction in whole or in part is permitted for any purpose of the  
United States Government.

NO OTS

OFFICE OF NAVAL RESEARCH

Number 3511 (00)

Project Number 051 - 380

EXPERIMENTAL INVESTIGATIONS ON THE LIGHT SCATTERING OF COLLOIDAL SPHERES.  
V. DETERMINATION OF SIZE DISTRIBUTION CURVES BY MEANS OF SPECTRA OF THE  
SCATTERING RATIO

BY

W. HELLER, M. L. WALLACE, AND A. F. STEVENSON

TECHNICAL REPORT NO. 4 (50)

April 15, 1963

Submitted by

W. Heller, Project Director

Department of Chemistry

Wayne State University

Detroit 2, Michigan

Reproduction in whole or in part is permitted for any purpose of the  
United States Government.

TO BE SUBMITTED FOR  
PUBLICATION IN THE  
JOURNAL OF PHYSICAL CHEMISTRY.

EXPERIMENTAL INVESTIGATIONS ON THE LIGHT SCATTERING OF COLLOIDAL SPHERES.  
V. DETERMINATION OF SIZE DISTRIBUTION CURVES BY MEANS OF SPECTRA OF THE  
SCATTERING RATIO<sup>1</sup>.

Wilfried Heller and M. L. Wallach<sup>2</sup>

Department of Chemistry, Wayne State University, Detroit, Michigan

and

A. F. Stevenson

Department of Physics, Wayne State University, Detroit, Michigan

I. INTRODUCTION

The preceding paper in this series dealt with the scattering ratio,  $\sigma$ , determined at an angle of  $90^\circ$  with respect to the incident beam as a means for determining particle size from light scattering in monodisperse colloidal dispersions of non-absorbing spheres<sup>3</sup>. The principal advantages of the use of  $\sigma$  over a series of other possible light scattering techniques were found to be (a) its relative insensitivity to errors in concentration, (b) the fact that no instrument constant is needed and (c) its high prospective sensitivity to heterodispersion. In view of these advantages, the scattering ratio appeared very promising as an argument for determining size distribution curves in heterodisperse systems. An extensive theoretical investigation of this problem<sup>4</sup> laid the foundation for a practical application of  $\sigma$ -spectra to this end. The present paper is concerned with this practical application<sup>5</sup>. Its results apply equally to measurements of the depolarization (polarization ratio at  $90^\circ$ ).

1. This work was supported by the Office of Naval Research. The results given in the present paper were presented at the 134th meeting of the American Chemical Society; Chicago, September, 1958.
2. Present address: Film Department, E. I. DuPont & Co., Wilmington, Delaware.
3. W. Heller and R. Tabibian, J. Phys. Chem. 66, 2059 (1962).
4. A. F. Stevenson, W. Heller, and M. L. Wallach, J. Chem. Phys. 34, 1789 (1961).
5. Regarding other recent attempts at using light scattering for a determination of size distributions, reference may be made to the extensive literature review given in reference 4.

## II. BRIEF REVIEW OF THE THEORY

The theoretical variation of the scattering ratio  $\sigma$  with  $\alpha \propto r^6$  investigated previously<sup>7</sup> shows (Figure 1 to 3 in ref. 7) that its spectrum will exhibit a series of maxima and minima at constant particle size, their number being larger the wider the spectral range used. As shown more recently<sup>4</sup> these maxima and minima move to longer wavelengths and become shallower as the system becomes more and more heterodisperse. (See particularly Figure 5 and 6 in ref. 4).

In order to correlate the spectral location of  $\sigma$ -maxima and minima and the amplitude of the spectral oscillations of  $\sigma$ , with size distribution curves, a certain basic type of distribution curve must be assumed unless the accessible spectral range is extraordinarily wide or unless a series of additional light scattering criteria are used. Instead of using any of the various possible well-known distributions, such as Gaussian, log normal, Maxwellian, a special type of distribution was assumed in the present work: a distribution which fitted well those found in emulsions. The reason for this is that colloidal emulsions most likely will represent one of the most important areas where this new technique is valuable since electron microscopy cannot be applied here except under very special circumstances. The distribution function selected is

$$f(r) = (r-r_0) \exp \left\{ - [(r-r_0)/s]^3 \right\}, \quad r \geq r_0, \quad (1) \\ = 0, \quad r < r_0.$$

where  $Cf(r) dr$  is the number of particles per unit volume with radii between  $r$  and  $r + dr$ ,  $C$  is a normalization constant, and  $r_0$  and  $s$  are parameters characterizing the distribution;  $r_0$  is the radius of the

---

6.  $\alpha = 2\pi r^3/\lambda$  where  $r$  is the radius of the sphere and  $\lambda$  is the wavelength in the surrounding medium.

7. W. Heller, W. J. Pangonis, and N. A. Economou, J. Chem. Phys. 34, 971 (1961).

smallest particle present in consequential numbers while  $s$  determines the modal radius  $r_m$ , the half width  $w$ , and the "half spread"  $(r_m - r_0)$  of the distribution through the relations

$$w = 0.9015 s \quad (2)$$

$$r_m - r_0 = s^{-1/2} s \quad (3)$$

The type of distribution curve represented by eq. (1) is similar to a log-normal distribution inasmuch as it is positively skewed as generally found in colloidal systems. It differs from it and from any other distribution curve by the fact that it generally begins at a finite  $\alpha$  (at a finite particle size). This has two reasons: First, particle size distributions within the Rayleigh range ( $\alpha \leq 0.4$ ) cannot be determined without additional criteria, the respective section of an optical distribution curve being therefore meaningless irrespective of the type of distribution assumed. Secondly, and most importantly, the smallest limiting particle size determined with this type of function represents well the number of particles present in consequential numbers. This therefore introduces an additional practically useful parameter for the characterization of particle size distributions.

In heterodisperse systems, the scattering ratio is

$$\sigma' = \int_0^\infty J_{//} C(r) dr / \int_0^\infty J_{\perp} C(r) dr \quad (4)$$

Here  $J$  is intensity of light scattered, at an angle of  $90^\circ$  with respect to the incident beam, by a single particle of radius  $r$ , per unit solid angle and unit intensity of the incident beam. On changing the variable from  $r$  to  $\alpha$

$$\sigma' = F_{//}(p, q) / F_{\perp}(p, q). \quad (5)$$

The quantities  $p$  and  $q$  are defined by

$$p = 2r_0 \pi / \lambda, \quad (6)$$

$$q = 2s \pi / \lambda. \quad (7)$$

The  $\sigma$ -values corresponding to all p and q values that may practically be encountered in colloidal dispersions of non-absorbing spheres have been tabulated for the relative refractive indices  $m = 1.05$  (0.05)  $1.30^8$  using as a theoretical basis the Mie-theory<sup>9</sup>.

For practical work it is convenient to normalize the data with respect to the green mercury line as the reference wavelength,  $\lambda_R$ . In the present work, where the dispersing medium is water at  $25^\circ$ ,  $\lambda_R = 4093.57\text{\AA}$ . The corresponding normalized p and q values

$$p_R = 2\pi r \lambda_R \quad (8)$$

$$q_R = 2\pi r / \lambda_R \quad (9)$$

As already shown<sup>4</sup> the practically important quantities

$$w = 0.05873 q_R, \quad (10)$$

$$r_m - r_o = 0.04517 q_R, \quad (11)$$

$$r_m = 0.04517 q_R + 0.06515 p_R, \quad (12)$$

$$r_o = 0.06515 p_R \quad (13)$$

The actual procedure in deriving distribution curves consists of the following steps: (1) spectra of the scattering ratio are obtained at various concentrations; (2) the spectrum pertinent to infinite dilution is derived; (3) a few exploratory theoretical spectra are derived for several pairs of  $p_R$  and  $q_R$ -values; (4) the exact  $p_R$  and  $q_R$  values are decided upon

---

8.  $m = \mu_2 / \mu_1$ , where  $\mu_2$  is the refractive index of the spheres and  $\mu_1$  that of the medium.

9. Tables of Scattering Functions for Heterodisperse Systems, A. F. Stevenson and W. Beller; Wayne State University Press; Detroit, Michigan, 1961.

which will give the best possible fit of the theoretical and experimental spectrum. A number of variations of this basic principle are possible and have been discussed<sup>6</sup>.

In the present work, the theoretical spectra giving the best fit were obtained by means of hand calculations, in order to get as intimate a knowledge of the sensitivity of the theoretical spectra to  $p_R$  and  $q_R$  as possible. In systematic practical application of the method, the fitting procedure by means of electronic computer is obviously indicated on account of the considerable amount of time that thus can be saved. Steps (3) and (4) are then reduced to a single operation.

### III. EXPERIMENTAL

#### 1. The Systems Investigated

The experimental tests were carried out on heterodisperse latices of polystyrene, obtained by selectively mixing portions of eighteen relatively monodisperse latices. The mean particle size of the monodisperse latices varied systematically from 758 to 1,300 m $\mu$ <sup>10</sup> in intervals of about 30 m $\mu$ . Therefore smooth distribution curves of almost any type could be obtained by proper mixing. The polystyrene systems-in which  $m$  closely approximates 1.20 at 5461A-were attractive also because the light scattering of monodisperse polystyrene latices had already been investigated extensively<sup>11</sup>. Three heterodisperse systems were thus prepared, one in which the distribution approximated that given by Equation 1 (H.D.1.), a second in which the distribution was antisymmetrical i.e. negatively skewed, (H.D. 2.) and a third which was approximately Gaussian, (H.D. 3).

Each of the 3 prepared stock mixtures had a concentration of 10 g of polymer per 1,000 g latex. From each of them a series of dilution were made so that the  $\sigma$ -spectra could be extrapolated to zero concen-

- 
10. The monodisperse samples were kindly provided by Dr. J. W. Vanderhoff of the Dow Chemical Company.
  11. R. M. Tabibian, W. Heller, and J. M. Epel, J. Coll. Sci. 11, 195 (1956) and later papers, *ibid*.



tration. The highest and lowest concentration optically investigated within these three dilution series were  $\leq 1.40 \times 10^{-4}$  and  $(5-8) \times 10^{-5}$  g of polymer per 1,000 g of latex. For technical details, reference may be made to the investigations on monodisperse systems since they were identical except for the following: Centrifuging was omitted and, prior to filtering, stabilizer was added and ultrasonic irradiation carried out for 10 minutes. This was found to effectively disperse any aggregates that may have been present.

## 2. The Optical Measurements

The apparatus described previously<sup>3</sup> was used for the present work also after applying the following modifications: (1) A 150 candle power a.c. Pointolite arc lamp was employed as an incandescent light source since it combined high brightness at all wavelengths in the visible with virtually constant output. (2) Among the various diaphragms used in the apparatus (See Fig. 1 in reference 3) the following were increased in aperture:  $A_7$  (4  $\rightarrow$  5.4 mm.),  $D_9$  (4.0  $\rightarrow$  5.2 mm.),  $D_{10}$  (4.1  $\rightarrow$  5.4 mm.). As done previously  $D_{12}$  (6.7 mm.) was generally omitted.

The spectra were investigated between the limiting wavelengths of 4510 and 5970A for H.D.1 and 2, and between 4540 and 6000A for H.D.3. In order to increase the intensity of the incident beam, a slightly larger entrance slit to the monochromator A (see fig. 1<sup>3</sup>) was used than previously. The resulting increase in the low intensity polychromatic background of the narrow spectral band emerging from the monochromator was largely compensated, however, by passing the light beam, prior to its entry into the monochromator, through colored aqueous solutions<sup>12</sup>. The width of the spectral band obtained from the monochromator and its variation with wavelength will be taken into account in the results to be discussed below<sup>13</sup>.

---

12. These solutions, acidified if necessary, contained two or more components of the following salts in a suitable concentration:  $\text{Cu}(\text{NO}_3)_2$ ,  $\text{Cr}(\text{NO}_3)_3$ ,  $\text{CuCl}_2$ ,  $\text{K}_2\text{Cr}_2\text{O}_7$ ,  $\text{Co}(\text{SO}_4)$ , and  $\text{NiCl}_2$ .

13. The width of the spectral band entering the apparatus varied between the blue and the orange from 11 to 32, 5 to 12, and 6 to 16 millimicrons in the experiments with H.D.1, H.D.2, and H.D.3, respectively. The more important half width of the intensity distribution throughout the spectral band, which is decisive for the response of the photocell, was of course considerably smaller, but it is the former which will be used in determining the maximum uncertainty of the results.

The solid angle  $\omega$  controlled by the position of diaphragm D12 was varied within a relatively narrow range depending on the scattered intensity<sub>3</sub> required for a measurement. It had a minimum value of  $1.23 \times 10^{-3}$  and a maximum value of  $9.6 \times 10^{-3}$  steradians. The latter was used in the majority of measurements. This compares with the standard solid angle of  $1.5 \times 10^{-3}$  steradians used previously. This angle was still within the range where the value of the scattering ratio is not affected as yet<sup>3</sup>.

The anisotropy of the photomultiplier tube was determined quantitatively by special experiments and was taken into account in the numerical data of  $\sigma^{14}$ .

The actual determinations of the scattering ratio were carried out according to the detailed technique described previously<sup>3</sup>.

### 3. Electron Microscopy

In view of the mixing procedure used, the synthetic size distribution curve was, of course, a priori known. Nevertheless, an electron microscopic analysis of the final mixtures was also carried out. The optical data to be reported below are checked against these alternate results<sup>15</sup>. The analysis of the electron photomicrographs was carried out on their projections onto a large screen giving an overall magnification of 140,000. Only the central portions of the individual micrographs were considered in order to eliminate the effect of minor distortions in the peripheral sections which may not necessarily be apparent visually. In order to be absolutely certain of the results

---

14. The anisotropy may be expressed in terms of  $d_{//}/d_{\perp}$ . Here  $d$  is the actual deflection of the galvanometer in the absence of any scattering solution with the photomultiplier tube mounted with its long axis in the plane of observation, its customary position in the apparatus used. The subscripts  $//$  and  $\perp$  pertain to an incident polarized beam vibrating parallel and perpendicular, respectively, to the plane of observation. The ratio varied from 0.964 to 0.971 between 4500 and 6000 Å. viz., by only 0.7% over the entire spectrum used.

15. The electron photomicrographs were kindly provided by Dr. J. H. L. Watson of the Edsel B. Ford Institute for Medical Research, Detroit, Michigan.

for H.D.1 and H.D.2, all particles in the central section considered were, in addition, measured in two orthogonal directions and all those results were rejected in which the axial ratio differed from unity by more than 5%.

#### IV. RESULTS

##### 1. Distribution Curve of the Type Given by Eqn. 1.

The small black discs in Fig. 1 represent the most probable values of the  $\sigma$ -data obtained experimentally on H.D.1. The rectangle within which the most probable value is contained or horizontal line which passes through it give the extreme limits in the uncertainty of these data. The exact width of the band of incident radiation<sup>13</sup> is indicated by the horizontal dimension of the rectangle (length of the line) while the maximal uncertainties in the numerical value of  $(I_{//}/I_{\perp})_0$  (The subscript 0 signifies extrapolation to zero concentration) are represented by the height of the rectangle. Among all possible theoretical curves which fit the experimental data on varying  $p_R$  and  $q_R$  in steps of 0.2, the choice could be narrowed down to the set of four lightly drawn or dashed curves given. These curves were calculated from Eq. 6 in Ref. <sup>16</sup>. They pertain to the parameters  $(p_R, q_R)$  of (6.8, 1.4), (6.8, 1.6), (7.0, 1.4), (7.0, 1.6). By interpolation between the four curves one can find one which fits the experimental data most closely; this curve, corresponding to  $p_R = 6.84$ ,  $q_R = 1.49$ , is represented by Curve I in Fig. 1. It gives the fully drawn distribution curve in Fig. 2. (The ordinate  $Cf(r)$  is, as stated, proportional to the number of particles, per unit volume, whose radius is  $r$ .)

---

16. The theoretical data were calculated assuming that  $m = 1.20$  over the entire spectral range. The dispersion of  $m$ , which should be taken into account when significant, was found not to alter the general pattern of the results here and could therefore be neglected.

The electron microscopically obtained histogram of the distribution curve (analysis of 982 particles) is also shown in Fig. 2<sup>17</sup>. In view of the expanded scale of the abscissa, the agreement must be considered as very satisfactory. The peak of the distribution curve representing the modal diameter ( $D_m$ ) as obtained by the two methods differs by 5%, the half width, by 22%, the "half spread"  $2(r_m - r_o)$  by only 2% and the smallest particle diameter  $D_o$  by 6%. The theoretical curve in Fig. 1 which satisfied the experimental data the least ( $p_R = 7.0$ ,  $q_R = 1.6$ ) gives the dashed distribution curve II in Fig. 2. It is readily seen that it does not differ much from the distribution curve obtained by interpolation. Hence, one may dispense with interpolation<sup>18</sup> if optimum accuracy is not essential.

## 2. Negatively Skewed Distribution Curve

The experimental data for H.D.2 (distribution curve anti-symmetrical to that postulated by Eq. 1) are given in Fig. 3. The theoretical curve which comes closest to an acceptable fit with the experimental data is obtained by interpolation between 4 pairs of  $p_R$  and  $q_R$  values. The parameters of this Curve (I),  $p_R = 8.15$ ,  $q_R = 0.85$ , yield the normalized distribution curve I in Fig. 4. Comparison with the electron microscopic histogram shows that the number distribution obtained is quantitatively not satisfactory. It is noteworthy, however, that the derived distribution function does, even in this case, reproduce the electron microscopic modal diameter to within 4%.

---

17. The optical distribution curve is normalized with respect to the electron microscopic histogram so that they each subtend equal areas. This procedure was adopted with all the systems investigated.

18. Normalization of both experimental and theoretical data represented in Fig. 1 with respect to the data at the reference wavelength may facilitate the analysis and in favorable cases improve the accuracy of the results.

The fact that the distribution curve obtained from light scattering deviates here from the actual one is of course not surprising. Indeed, it is very gratifying to see from Fig. 3 as compared to Fig. 1 that a radical deviation of the distribution curve from that assumed manifests itself immediately by the fact that no theoretical spectrum can be found which satisfies the experimental one in satisfactory approximation over a sufficiently extensive spectral range. The risk of obtaining fictitious distribution curves from light scattering spectra is therefore quite small since the impossibility of a satisfactory fit between theoretical and experimental spectra represents an automatic check.

The question naturally arises as to what may usefully be done in absence of a satisfactory fit. The possibilities of resolving the problem will be discussed in section V with emphasis upon one possibility adopted in the present work.

### 3. Gaussian Distribution

Considering, finally, H.D.3 with its normal distribution curve, Fig. 5 gives the experimental  $\sigma(\lambda)$  data and, in addition, the interpolated best fitting theoretical  $\sigma(\lambda)$ -curve characterized by  $p_R = 5.65$ ,  $q_R = 1.90$ . The size distribution obtained from this best  $\sigma(\lambda)$ -curve is compared with the electron microscopic histogram in Fig. 6. The modal diameters agree to within 5% which is, like in the case of H.D.1 and 2, within the uncertainty of the electron microscopic histogram. The half width agrees to within 27%, and the value for the smallest particles present in consequential numbers to within 14%. Normal distribution curves can, therefore, be analysed satisfactorily with the method outlined. The deviations of the best fitting theoretical spectrum from the experimental spectrum are distinct, but considerably smaller than in the preceding instance (H.D.2). Therefore, very precise experimental data are necessary in order to give a clear indication-as apparent from Fig. 5-that the distribution curve is not fully in line with that assumed.

V. DETERMINATION OF SIZE DISTRIBUTION CURVES WHEN THEORETICAL AND EXPERIMENTAL  $\zeta$ -SPECTRA DO NOT MATCH SATISFACTORILY.

In absence of a satisfactory fit between theoretical and experimental  $\zeta$ -spectra-which indicates non-compliance of the actual distribution curve with that assumed, one has the choice between four possibilities, three of which have already been briefly discussed<sup>4</sup>.

(1) A first approximation method based on graphical interpolation.

The size distribution curves for H.D.1, H.D.2, and H.D.3 were obtained by interpolation for the proper  $p_R$  and  $c_R$  values from four of those  $\phi(\lambda)$  curves which came closest to satisfying the experimental data. An alternate method since then adopted consists of picking two curves only, selected in such a manner that all experimental points are, throughout the entire spectrum, contained within the area between the two curves. One thus establishes two distribution curves. While they differ very little if the actual distribution curve is of the positively skewed type, i.e. if the area between the two theoretical spectra is very small, an appreciable difference is found in other circumstances. Graphical interpolation between the two curves yields then a distribution curve approximating that of the system. This interpolated curve clearly deviates from the type given by eq. (1). It may, in extreme cases be primarily negatively skewed or even bimodal<sup>19</sup>.

(2) A-second approximation method based on the use of a two term equation.

As already pointed out previously<sup>5</sup>, the rigidity with which the basic type of distribution is fixed by eq. (1) can be removed by adding a

---

19. Since in practical large scale application of the methods outlined here, computer fitting of theoretical and experimental spectra is highly desirable; the procedure to be adopted in the present instance is the independent match of two halves of the spectrum and a subsequent match of the entire spectrum. If the minimal sum of the absolute deviations (or of their squares) from the experimental data has in all three instances approximately the same value, eq. (1) applies. Otherwise, the computer will have to be ordered to derive from the two complete spectral curves the arithmetic mean. The latter result is that corresponding to the first approximation method outlined.

second term. This gives

$$\begin{aligned} g(r) &= f(r, r_0, s) + (C/C_1) f(r, r'_0, s') \\ &= (r-r_0) \exp \left\{ -[(r-r_0)/s]^3 \right\} + (C_2/C_1) (r-r'_0) \exp \left\{ -[(r-r'_0)/s']^3 \right\} \end{aligned} \quad (14)$$

This equation was applied to H.D.2, using analytical principles discussed previously<sup>4</sup>. The heavily drawn curve II in Fig. 3 shows the theoretical  $\sigma(\lambda)$  curve thus obtained and the heavily drawn curve II in Fig. 4 represents the resulting distribution. It agrees satisfactorily with the electron microscopic histogram. In particular, the number distribution is essentially correct and, in addition, the tail towards the small particle size range is reproduced satisfactorily. It will be noted that the modal diameter is the same as before [on using rather eq. (1)]. The only unavoidable artifice introduced by the second term is the sudden change in slope which occurs in the present instance between  $D_0$  and  $D_m$ . In practical application, it would be reasonable to smooth out such a kink.

On using the two term equation, it is necessary to know the individual theoretical values of  $I_{//}$  and  $I_{\perp}$  or  $KI_{//}$  and  $KI_{\perp}$  where  $K$  is a constant at a given wavelength. This information is included in the tables referred to above<sup>9</sup>.

The task of finding the proper  $p_R$  and  $q_R$ -values can be simplified considerably by using the two limiting distribution curves established according to the first approximation procedure discussed above (V, 1). Any of the two curves provides the  $p_R$  and  $q_R$  values while the other provides the  $p'_R$  and  $q'_R$  values. The proper  $C_2/C_1$  is found by successive approximation, but, in general, no error of consequence will be committed on assuming that  $C_2/C_1 = 1.0$ .

### (3) Other Possibilities

Two further possibilities, which already have been discussed briefly are at present under investigation, but no statement can be made as yet on their practical advantage over the 2 preceding procedures.

First of all, one may, in absence of a satisfactory fit, test the ex-

perimental  $\sigma$ -spectrum successively against theoretical spectra resulting from 2 or 3 characteristically different theoretical prototypes of distribution functions. This procedure makes the use of an electronic computer mandatory.

The second additional possibility which-theoretically at least-is the most attractive one consists of deriving from scattering data a distribution curve without making any assumption whatsoever about its character. While this is, in principle possible, it is necessary to increase the number of experimental data considerably if a single valued answer is to be obtained. In other words, in addition to  $\sigma$ -spectra, turbidity spectra (discussed in a subsequent paper) and the variation of scattering with the angle of observation must be included as experimental arguments.

VI. Simplification of Procedure If the Objective is Merely  
The Determination of the Peak of The Distribution Curve  
Or of the Number Average Particle Size.

For many purposes, particularly in industrial control work, it is less important to know all the details of a particle size distribution than it is to determine the particle diameter,  $D_m = 2r_m$  at which the distribution has its peak (modal diameter) or the number average particle diameter,  $\bar{D}_n$ . The simplifications which are then possible in the procedures described become apparent on the basis of Table I. It lists in the first row  $D_0 (=2r_0)$  and  $D_m$  as obtained for all three systems from  $\sigma$ -spectra using eqn. (1). The percent deviation of the results relative to electron microscopic determination is given in parentheses. (The deviation is considered positive if the light scattering value is larger)<sup>20</sup>. The second row contains the corresponding data obtained on using the two term eqn. (14) for H.D.2.

It is seen that the deviation in  $D_m$  is throughout within the limits of uncertainty of electron microscopic measurements (about 5%) even on

---

20. The deviations were evaluated by means of polygons inscribed in the histograms of Fig's. 2, 4, and 6. They were erased prior to reproduction of these figures.



TABLE I

Values in millimicrons, of  $D_o$  and  $D_m$ , as obtained from  $\sigma$ -spectra on using one-term equation (1), two term equation (14) and from  $\sigma$ -value at the single wavelength of 5460.73A. Percent deviation relative to electromicroscopic values are given in parentheses.\*

	H.D.1		H.D.2		H.D.3	
	$D_o$	$D_m$	$D_o$	$D_m$	$D_o$	$D_m$
Eq. (1)	890 (-6)	1030 (-5)	1062 (16.2)	1140 (4)	736 (14)	910 (5)
Eq. (14)	-	-	964 (5.5)	1140 (4)	-	-
5460.73A.	-	1070	-	1100	-	940

\*The electromicroscopic value of  $D_o$  is defined here as that diameter which is exceeded by 99% of all particles present in the system.

applying eqn. (1) to a system with a characteristically different distribution curve (H.D.2). A very rough fit of experimental and theoretical  $\sigma$ -spectra is therefore sufficient in order to obtain a satisfactory value for  $D_m$ . This is simply due to the fact that

$$D_m = 0.093034 q_R + 0.13030 p_R \quad (15)$$

i.e.  $D_m$  varies only slowly with  $q_R$  and  $p_R$ . Thus, the four distribution curves derived from the four theoretical spectra in Fig. 1 differ in  $D_m$  by less than 2%. This fact and, particularly, the very satisfactory  $D_m$  value obtained for H.D.2 shows also clearly that coincidence of  $D_m$  obtained both by light scattering and by another method is no guarantee whatsoever that the distribution curve assumed applies to the system under investigation. It is important to note that this applies, of course, also to other possible experimental criteria, such as turbidity spectra or angular variation of scattering and to the use of other theoretical distribution functions. In contradistinction to  $D_m$ , the value of  $D_0$  is very sensitive to the type of distribution assumed as apparent from the data of H.D.2 and H.D.3 as compared to H.D.1<sup>21</sup>.

The statements made with regard to  $D_m$  apply, in a first approximation, also to the number average particle diameter,

$$\bar{D}_n = 0.06515 (1.476 q_R + 2.000 p_R) \quad (16)$$

as the similarity of the numerical coefficients in eqns. (15) and (16) indicates.

A particularly simple situation arises if  $p_R$  is appreciably larger than  $q_R$ . It follows then from eqn. (15) and (16) that, in a first approximation  $D_m$  and  $\bar{D}_n$  respectively are directly proportional to  $p_R$ . In other words, it is then possible to derive  $D_m$  ( $\bar{D}_n$ ) from a single measurement at the reference wavelength. This is tested in the third row of Table I for  $D_m$ . These data are simply obtained from measurements

---

21. The electron microscopic value of  $r_0$  was obtained by discounting those smallest particles whose total number was less than 1 per cent of all the particles.

at the green Hg - line on associating with the  $\sigma$ -value that diameter which would obtain if the system were monodisperse. (For this purpose the theoretical data given in reference 7 were used). The error relative to the rigorous  $D_m$ -values in row one of Table I is clearly 4-5% throughout. Consequently, this procedure is quantitatively acceptable up to a  $q_R/p_R$  ratio of about 0.35. This means, in practical terms, a distribution curve whose half width is not more than about one third as large as the smallest particles present in consequential numbers. Thus, if, for instance, a distribution starts effectively at about 0.5 microns,  $D_m$  (and  $\bar{D}_n$ ) will be obtained from a single monochromatic measurement with an error not in excess of 5% if the halfwidth is not in excess of 160 millimicrons. This is essentially equivalent to requiring that no particles should be present in consequential numbers below 500 millimicrons nor above 800-850 millimicrons.

If  $q_R$  is appreciably larger than  $p_R$ ,  $D_m$  and  $\bar{D}_n$  will, in a first approximation be proportional to  $q_R$ , again according to eqs. (15) and (16). Therefore in strongly heterodisperse systems in which significant numbers of particles are present even within the lowest section of the colloidal range, the approximate value of  $D_m$  ( $\bar{D}_n$ ) obtained at a single wavelength is, in first approximation a relative measure of the degree of heterodispersion of the system.

#### VII. THE RANGE OF PRACTICAL USEFULNESS OF THE LIGHT SCATTERING METHOD IN CONNECTION WITH THE PROBLEM OF SIZE DISTRIBUTIONS.

One of the most attractive features of size distribution determinations from light scattering is the fact that the systems under investigation are not interfered with, in contradistinction to all other known methods. From the theoretical<sup>4</sup> and experimental investigation-including experimental evidence obtained after conclusion of the present work<sup>22</sup> it follows that the singlevaluedness and accuracy of data obtained from scattering depends on the spread of the distri-

---

22. Data obtained in this laboratory by Rodney Wu, and, more recently, by Bettye Greene (to be published later).

bution curve and on the size of the smallest particles present in consequential numbers. The role of the latter is relatively minor. From Fig. 2 (ref. 4), it follows that the sensitivity of the method should increase with  $p$ . On using visible light, an optimum can, however, be expected at a particle diameter in excess of several microns since then the number of maxima and minima per unit spectral range becomes too large to be measured conveniently. The width of the distribution curve, on the other hand, is far more important; Fig. 3 (ref. 5) shows that at  $q$ -values  $> 2.5$ ,  $\sigma$  varies, at constant  $p$ , only slowly and nearly linearly with  $q$ . The sensitivity of the method is therefore optimal at  $q$ -values  $< 2.5$ . This corresponds to a distribution curve with a half width not in excess of about 200 millimicrons, and an entire spread not in excess of about 400-500 millimicrons, if visible light is used<sup>23</sup>.

It follows from Fig. 3 that for  $q > 2.5$ , at a given  $\sigma$

$$Aq + Bp - Cpq \approx \text{constant} \quad (17)$$

so that in the absence of a numerically large spectral variation of  $\sigma$ , (maxima and minima being then essentially absent), a relatively large number of  $p$  and  $q$  combinations may satisfy the same spectrum. This problem is, clearly, not limited to the use of eq. (1) nor to the use of the experimental criterion used here ( $\sigma$ -spectra). It is bound to be encountered also on basing the analysis on other types of distribution or on using as experimental criteria turbidity spectra or the variation of scattering with the angle of observation. The lack of singlevaluedness of results to be expected, therefore, in very heterogeneous systems can be relieved, however, by using in addition to  $\sigma$ -spectra the two essentially equivalent criteria just named. A subsequent paper in this series will be concerned with this possibility.

---

23. The allowed spread increases in direct proportion to the wavelength. It is at least 1000 times larger at radar wavelengths.

## LEGENDS

Figure 1.  $\sigma$ -spectrum of H.D.1, a system conforming to the distribution assumed in equation (1).

black circles: most probable experimental value.

rectangles: maximum experimental uncertainty.

curves: theoretical spectra.

Figure 2. Size distribution curves of H.D.1.

I. Derived from best fitting interpolated theoretical  $\sigma$ -spectrum.

II. Derived from approximately fitting theoretical  $\sigma$ -spectrum.

Histogram: electron microscopic distribution curve.

Figure 3.  $\sigma$ -spectrum of H.D.2 (negatively skewed distribution).

I. Best possible theoretical  $\sigma$ -spectrum achieved by means of eq. (1).

II. Better theoretical  $\sigma$ -spectrum obtained on using equation (14).

Figure 4. Size distribution curve of H.D.2.

I. Using one-term equation (1).

II. Using two-term equation (14).

Figure 5.  $\sigma$ -spectrum of H.D.3 (Gaussian distribution).

Figure 6. Size distribution of H.D.3.

FIGURE 1

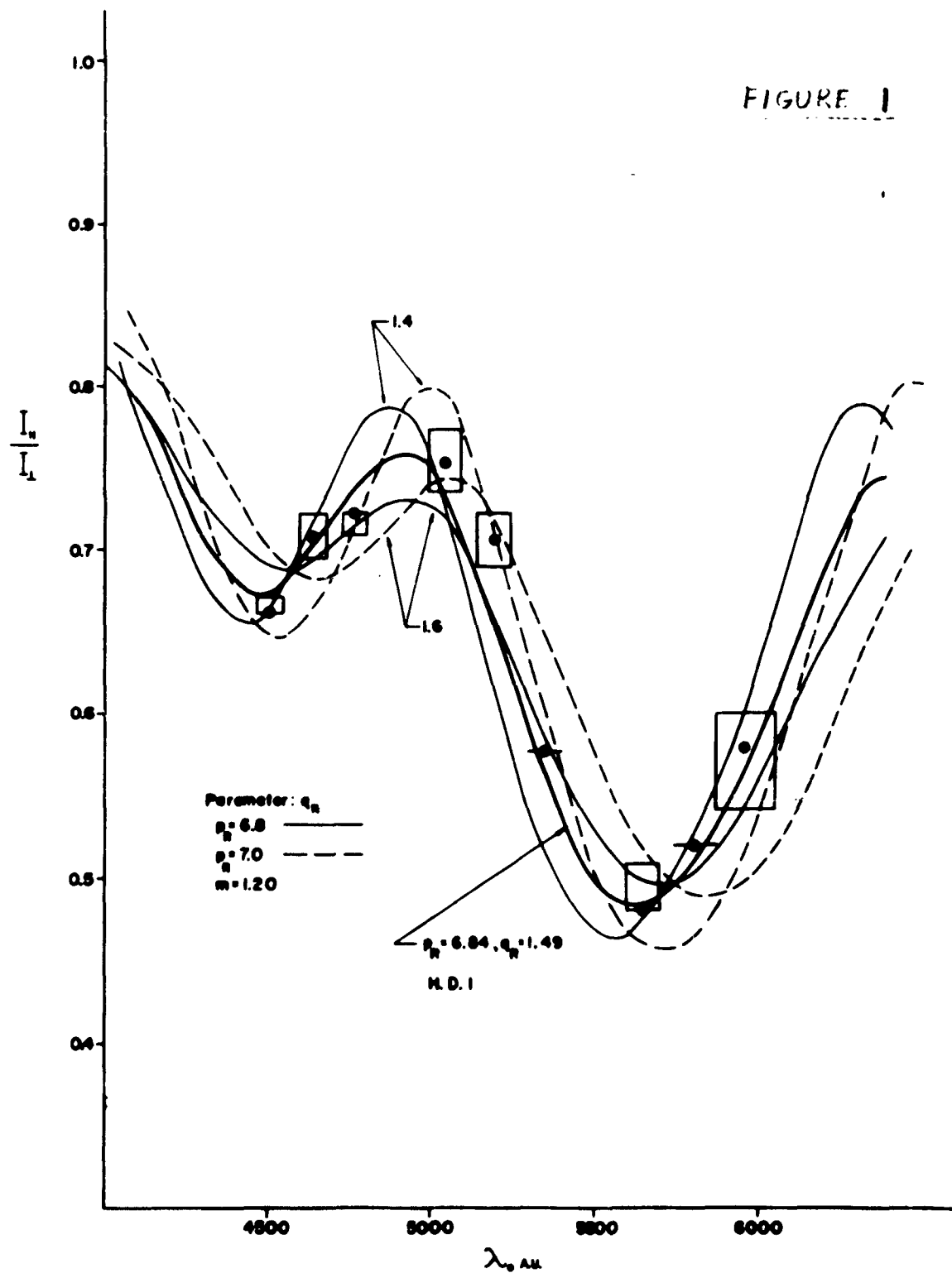
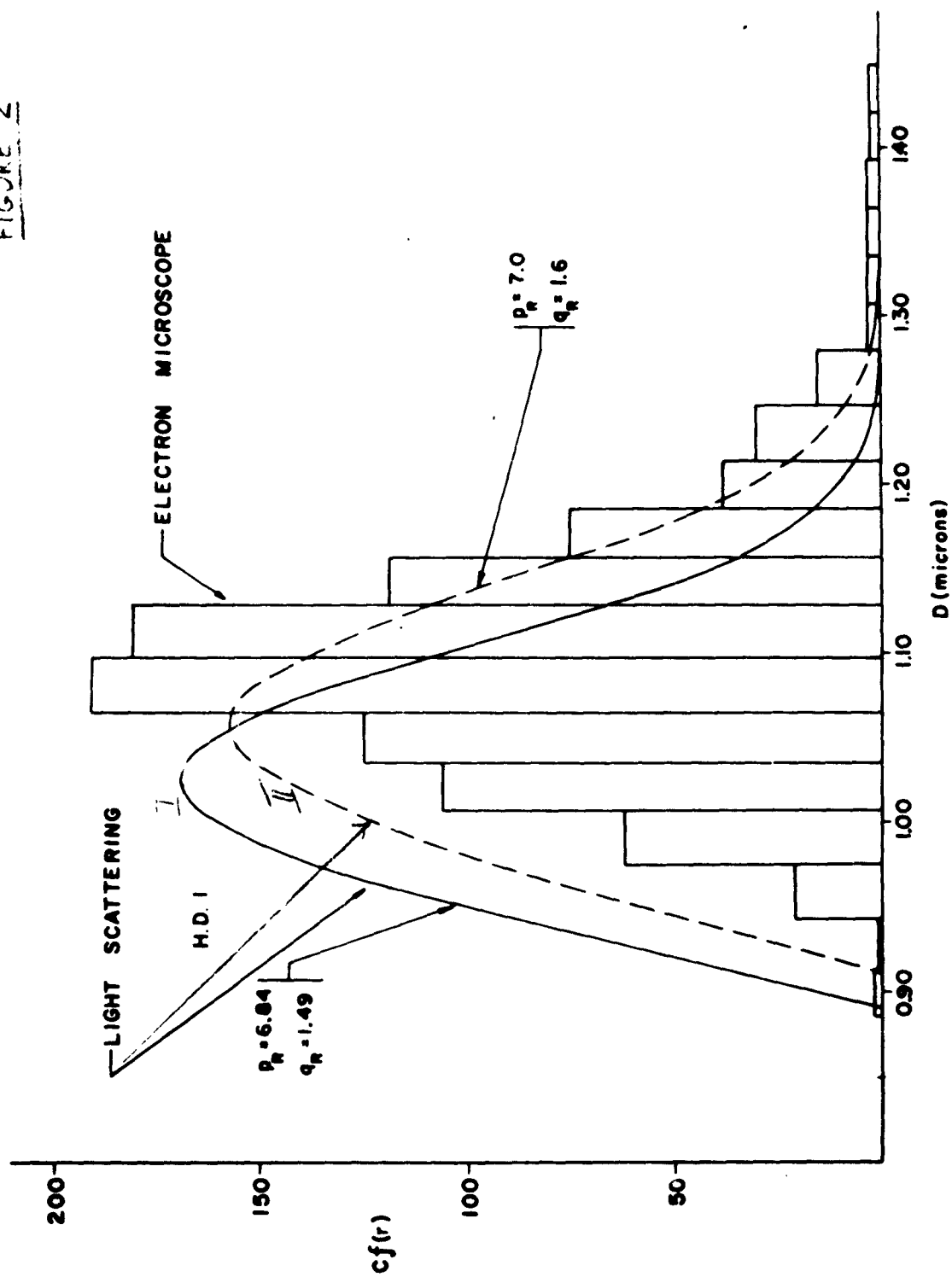


FIGURE 2



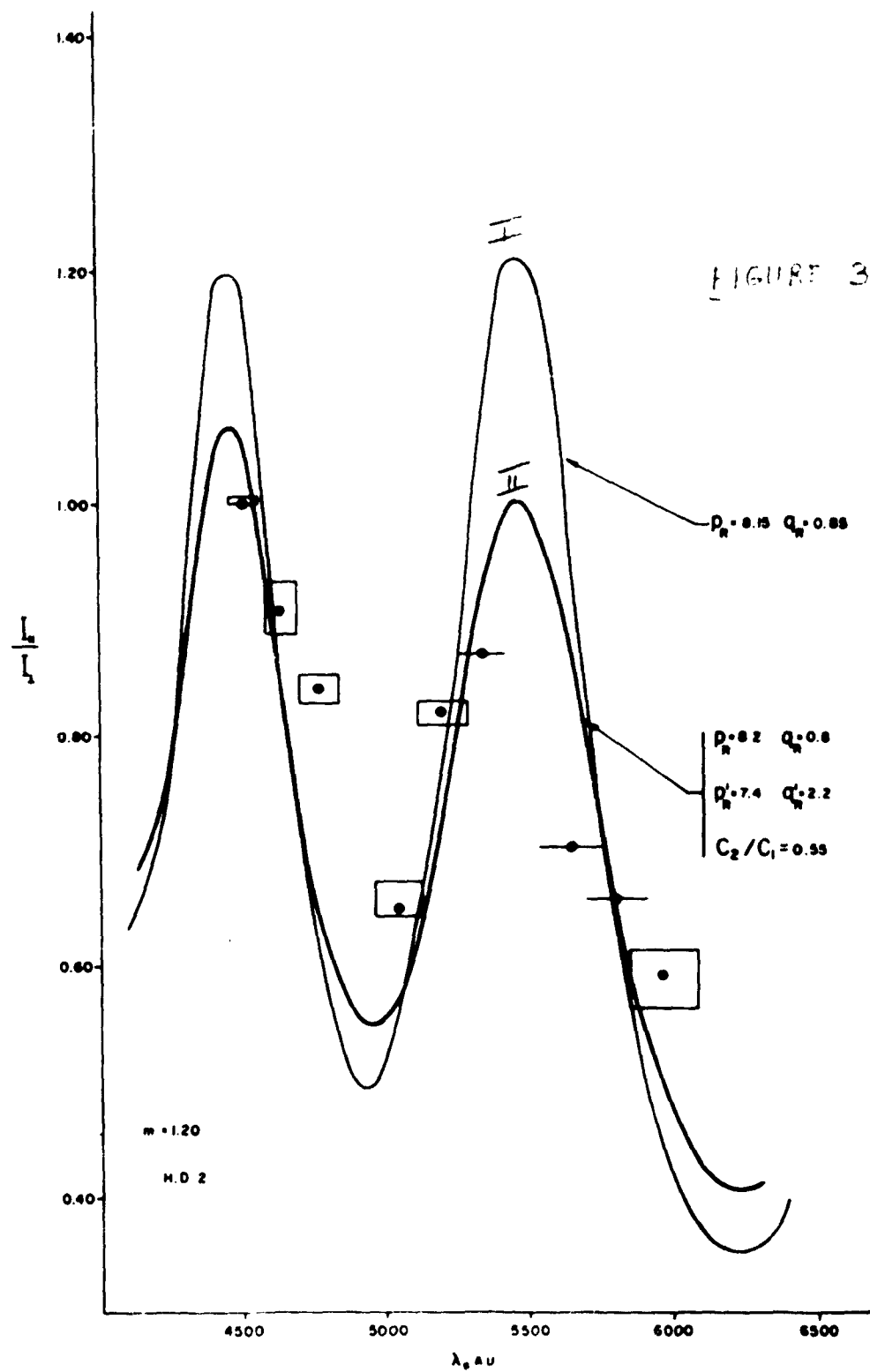
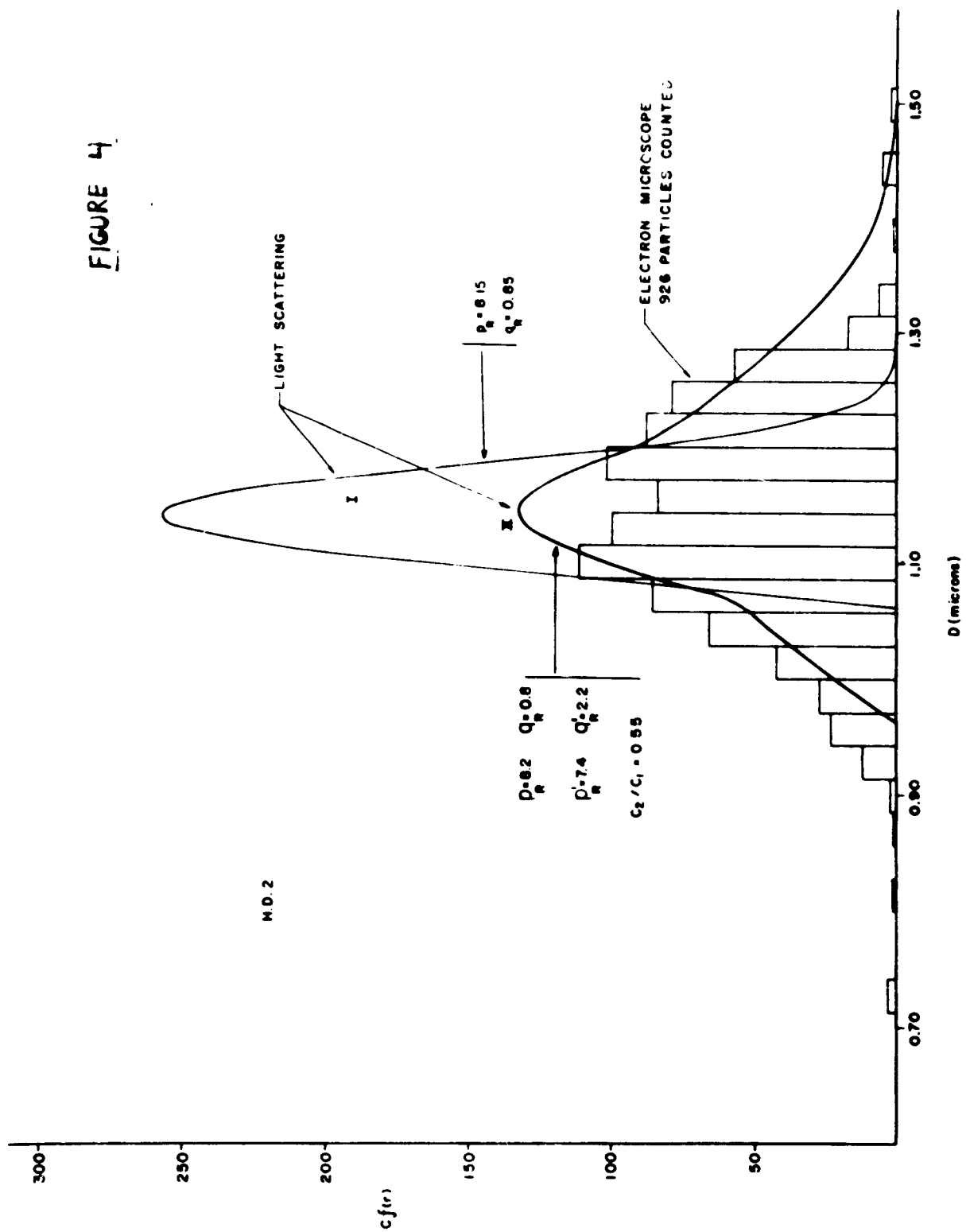




FIGURE 4



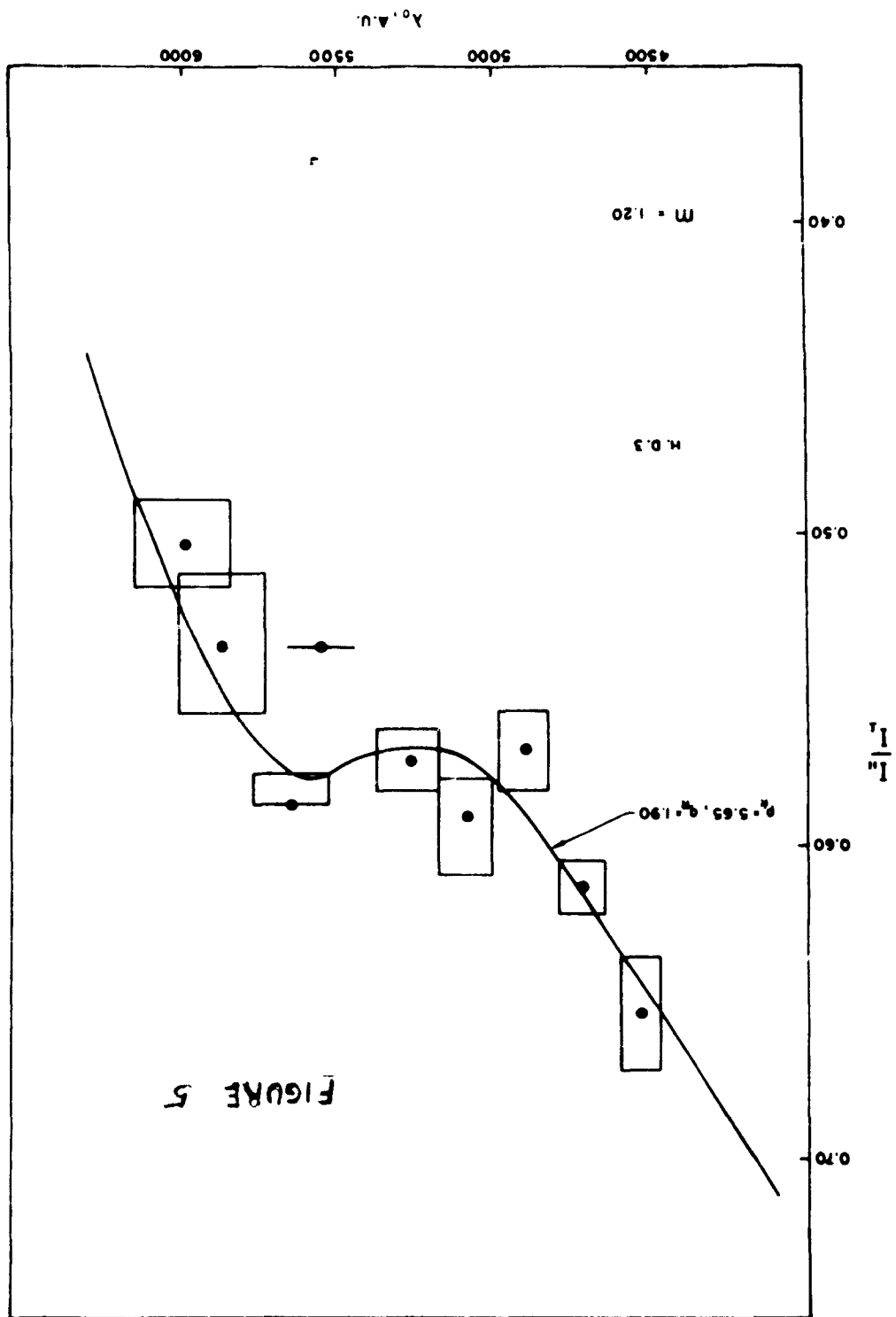
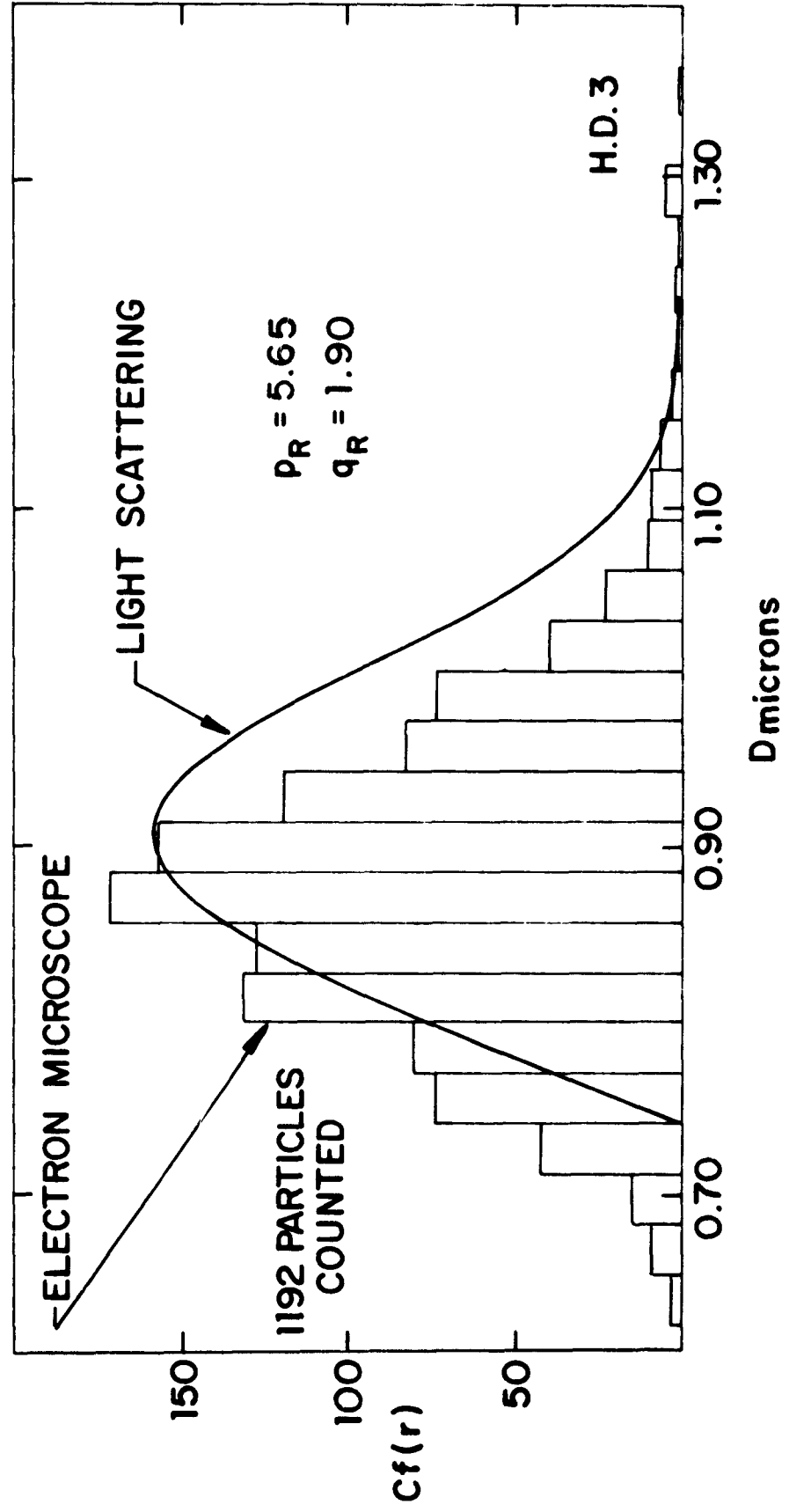


FIGURE 5

FIGURE 6



# TECHNICAL REPORT DISTRIBUTION LIST

Wayne State University

Contract Nonr 3511(00)

NR 051-380

	<u>No. Copies</u>		<u>No. Copies</u>
Commanding Officer Office of Naval Research Branch Office The John Crerar Library Building 86 East Randolph Street Chicago 1, Illinois	(1)	Air Force Office of Scientific Research (SRC-E) Washington 25, D. C.	(1)
Commanding Officer Office of Naval Research Branch Office 346 Broadway New York 13, New York	(1)	Commanding Officer Diamond Ordnance Fuze Laboratories Washington 25, D. C. Attn: Technical Information Office Branch 012	(1)
Commanding Officer Office of Naval Research Branch Office 1030 East Green Street Pasadena 1, California	(1)	Office, Chief of Research & Development Department of the Army Washington 25, D. C. Attn: Physical Sciences Division	(1)
Commanding Officer Office of Naval Research Branch Office Box 39 Navy #100 Fleet Post Office New York, New York	(7)	Chief, Bureau of Ships Department of the Navy Washington 25, D. C. Attn: Code 342 C	(2)
Director, Naval Research Laboratory Washington 25, D. C. Attn: Technical Information Officer (6) Chemistry Division	(2)	Chief, Bureau of Naval Weapons Department of the Navy Washington 25, D. C. Attn: Technical Library Code RRMA-3	(3) (1)
Chief of Naval Research Department of the Navy Washington 25, D. C. Attn: Code 425	(2)	ASTIA Document Service Center Arlington Hall Station Arlington 12, Virginia	(10)
DDR&E Technical Library Room 3C-128, The Pentagon Washington 25, D. C.	(1)	Director of Research U.S. Army Signal Research & Development Laboratory Fort Monmouth, New Jersey	(1)
Technical Director Research & Engineering Division Office of the Quartermaster General Department of the Army Washington 25, D. C.	(1)	Naval Radiological Defense Laboratory San Francisco 24, California Attn: Technical Library	(1)
Research Director Clothing & Organic Materials Division Quartermaster Research & Engineering Command U. S. Army Natick, Massachusetts	(1)	Naval Ordnance Test Station China Lake, California Attn: Head, Chemistry Division Code 40 Code 50	(1) (1) (1)

REVISED 1 FEB 1962

TECHNICAL REPORT DISTRIBUTION LIST

Page 2

Contract Nonr 3511(00)

Wayne State University

NR No. 051-380

	<u>No. Copies</u>		<u>No. Copies</u>
Commanding Officer Army Research Office Box CM, Duke Station Durham, North Carolina Attn: Scientific Synthesis Office	(1)	Aeronautical Systems Division ASRCNP Wright-Patterson Air Force Base Ohio	(1)
Brookhaven National Laboratory Chemistry Department Upton, New York	(1)	Office of Chief of Engineers Research and Development Division Department of the Army Gravelly Point Washington 25, D. C.	(1)
Atomic Energy Commission Division of Research Chemistry Programs Washington 25, D. C.	(1)	Engineer Research and Development Laboratory Fort Belvoir, Virginia Attn: Materials Branch, Mr. Mitton	(1)
Atomic Energy Commission Division of Technical Information Extension Post Office Box 62 Oak Ridge, Tennessee	(1)	Commander Mare Island Naval Shipyard Rubber Laboratory Vallejo, California	(1)
U.S. Army Chemical Research and Development Laboratories Technical Library Army Chemical Center, Maryland	(1)	Dr. J. H. Faull, Jr. 72 Fresh Pond Lane Cambridge 38, Massachusetts	(1)
Office of Technical Services Department of Commerce Washington 25, D. C.	(1)	Dr. R. S. Stein Department of Chemistry University of Massachusetts Amherst, Massachusetts	(1)
Dr. Albert Lightbody Naval Ordnance Laboratory White Oak, Silver Spring, Md.	(1)	Dr. L. F. Rahm Plastics Laboratory Princeton University Princeton, New Jersey	(1)
Dr. W. H. Avery Applied Physics Laboratory The John Hopkins University 8621 Georgia Avenue Silver Spring, Md.	(1)	Dr. A. V. Tobolsky Department of Chemistry Princeton University Princeton, New Jersey	(1)
National Bureau of Standards Washington 25, D. C. Attn: Chief, Organic and Fibrous Materials Division	(1)	Dr. U. P. Strauss Department of Chemistry Rutgers - The State University New Brunswick, New Jersey	(1)
Chief, Bureau of Yards and Docks Department of the Navy Washington 25, D. C. Attn: Code P300	(1)	Dr. Charles P. Roe Research and Development Department U. S. Rubber Company Passaic, New Jersey	(1)

## TECHNICAL REPORT DISTRIBUTION LIST

Page 3

Contract Nonr 3511(00)

Wayne State University

NR No. 051-380

	<u>No. Copies</u>		<u>No. Copies</u>
ONR Resident Representative University of Michigan Ann Arbor, Michigan	(1)	Dr. T. L. Heying Organics Division Olin Mathieson Chemical Corporation 275 Winchester Avenue New Haven, Connecticut	(1)
National Bureau of Standards Washington 25, D. C. Attn: Dr. Victor R. Deitz	(1)	Monsanto Research Corporation Everett Station Boston 49, Massachusetts Attn: Mr. K. Warren Easley	(1)
Commanding Officer Naval Air Development Center Johnsville, Pennsylvania Attn: Dr. Howard R. More	(1)	Dr. B. Wunderlich Department of Chemistry Cornell University Ithaca, New York	(1)
Plastics Technical Evaluation Center Pictinny Arsenal Dover, New Jersey	(1)	Dr. R. B. Fox Dr. J. E. Cowling Dr. D. L. Venezky Dr. A. L. Alexander Code 6120 Naval Research Laboratory Washington 25, D. C.	(1) (1) (1) (1)
Dr. G. Barth-Wehrenalp, Director Inorganic Research Department Pennsalt Chemicals Corporation Box 4388 Philadelphia 18, Pennsylvania	(2)	Mr. J. A. Kies Code 6210 Naval Research Laboratory Washington 25, D. C.	(1)
Mr. James P. Lodge, Chief Air Pollution Chemical Research Department of Health, Educ. and Welfare 4676 Columbia Parkway Cincinnati 26, Ohio	(1)	Mr. E. J. Kohn Code 6100 Naval Research Laboratory Washington 25, D. C.	(1)
Dr. T. G. Fox, Director of Research Mellon Institute 4400 Fifth Avenue Pittsburgh 13, Pennsylvania	(1)		
NASA 1512 H Street, N. W. Washington 25, D. C.			
Dr. M. S. Cohen, Chief Propellants Synthesis Section Reaction Motors Division Denville, New Jersey	(1)		
Dr. D. A. Brown Department of Chemistry University College Upper Merrion Street Dublin, Ireland	(1)		